



# De-excitation X-rays from resonant coherently excited 390 MeV/u hydrogen-like Ar ions

T. Ito <sup>a,\*</sup>, Y. Takabayashi <sup>a</sup>, K. Komaki <sup>a</sup>, T. Azuma <sup>b</sup>, Y. Yamazaki <sup>a,c</sup>, S. Datz <sup>d</sup>,  
E. Takada <sup>e</sup>, T. Murakami <sup>e</sup>

<sup>a</sup> *Institute of Physics, Graduate School of Arts and Sciences, University of Tokyo, 3-8-1 Komaba, Meguro, Tokyo 153-8902, Japan*

<sup>b</sup> *Institute of Applied Physics, University of Tsukuba, Tsukuba, Ibaraki 305-8573, Japan*

<sup>c</sup> *Atomic Physics Laboratory, RIKEN, Wako, Saitama 351-0198, Japan*

<sup>d</sup> *Oak Ridge National Laboratory, Oak Ridge, Tennessee 37830, USA*

<sup>e</sup> *National Institute of Radiological Sciences, Inage, Chiba 263-8555, Japan*

---

## Abstract

Resonant coherent excitation (RCE) of 390 MeV/u hydrogen-like Ar<sup>17+</sup> ions planar channeled in a Si crystal was investigated through measurements of the de-excitation X-rays as well as the charge state distribution of the transmitted ions. We observed enhancements of both the fraction of ionized Ar<sup>18+</sup> ions and the intensity of the de-excitation X-rays under the RCE condition. The  $n = 2$  states of Ar<sup>17+</sup> in the crystal are split into four energy levels due to spin-orbit interaction and Stark effect induced by the planar potential of the crystal. The intensities of the X-rays from the lower two levels were found to be smaller compared with those from the higher two levels, which is explained by the dominance of the 2s component not decaying via a single photon emission. The difference between the resonance profiles of the charge state and the X-ray reflects the nature of  $n = 2$  states in the crystal field. © 2000 Elsevier Science B.V. All rights reserved.

*PACS:* 61.85.+p; 34.50.Fa; 71.70.Ej

*Keywords:* Resonant coherent excitation; Channeling; Ionization of atoms; Spin-orbit interaction; Stark effect

---

## 1. Introduction

Channeled ions in a crystal have a possibility to be excited by feeling the periodic crystal potential as an oscillating electromagnetic field, when one of the internal energy differences of the ions corre-

sponds to the frequency of the field. This phenomenon called resonant coherent excitation (RCE) was predicted by Okorokov in 1965 [1,2]. Ions traveling in a target experience incoherent excitation or ionization by collisions with the target atoms. These processes under the channeling condition reduces compared with those for a random incidence. The once excited ions are either ionized or de-excited accompanying X-ray emission. Under the RCE condition, the coherent excitation and de-excitation processes are added to

---

\* Corresponding author. Tel.: +81-3-5454-6515; fax: +81-3-5454-6515.

*E-mail address:* ito@radphys4.c.u-tokyo.ac.jp (T. Ito).

the incoherent processes. An existence of the coherent excitation leads to increase both of ionization and X-ray emission.

The RCE of hydrogen-like and helium-like ions was first observed by Datz et al. [3] through the charge state distribution of the transmitted ions. Since then, much progresses in understanding of RCE are achieved [4,5]. The enhancement of de-excitation X-rays from  $n = 2$  states of  $\text{Ne}^{9+}$ ,  $\text{F}^{8+}$  and  $\text{Mg}^{11+}$  ions under the RCE condition in Au crystals was observed [6–9]. It was reported that the X-ray emission shows an anisotropy [9], and the resonance profile reflects the Stark split of the  $n = 2$  states originated in both the wake and crystal fields.

Recently, the first order RCE for  $1s$  to  $n = 2$  transition of 390 MeV/u hydrogen-like Ar ions in the Si ( $2\bar{2}0$ ) planar channeling was observed through the charge state of transmitted ions [10–12]. In the high energy region, the RCE is clearly observed, because incoherent electron loss and capture processes are much reduced. Moreover, the wake field is negligibly small compared with the static crystal field perpendicular to the ion velocity. A split of  $n = 2$  state was observed due to the spin-orbit interaction as well as the Stark effect originated in the static crystal field.

Excited ions have two decay channels, i.e., ionization and de-excitation. A study of both channels offers more detailed information on the RCE process. In the present paper, we report the RCE observation of 390 MeV/u  $\text{Ar}^{17+}$  ions under the Si ( $2\bar{2}0$ ) planar channeling condition through measurements of the de-excitation X-rays as well as the charge distribution of the transmitted ions.

## 2. Experimental

In the present experiment, an RCE was measured for the ( $2\bar{2}0$ ) planar channeling in a Si crystal. The condition is given by

$$\Delta E = \frac{\gamma\beta hc}{a} (\sqrt{2}k \sin\theta + l \cos\theta), \quad (1)$$

where  $\Delta E$  is a transition energy of the ion,  $\beta = v/c$ ,  $\gamma = 1/\sqrt{1 - \beta^2}$ ,  $v$  and  $c$  are the ion and

light velocities, respectively,  $h$  is the Planck's constant,  $a (= 5.431 \text{ \AA})$  is a lattice constant of a Si crystal. An angle from the  $[110]$  axis on the ( $2\bar{2}0$ ) plane is  $\theta$ , and  $k$  and  $l$  are integers. Keeping the ion velocity fixed, we scanned the tilt angle  $\theta$  across the  $(k, l) = (1, 1)$  resonance.

The experimental set-up is shown in Fig. 1. A beam of 390 MeV/u  $\text{Ar}^{17+}$  ions supplied from the Heavy Ion Medical Accelerator in Chiba (HI-MAC), was collimated so that the angular divergence and the beam diameter become to less than 0.15 mrad and 2 mm, respectively [11]. A Si crystal with 21  $\mu\text{m}$  thickness was mounted on a 3-axis goniometer. The ( $2\bar{2}0$ ) plane of the crystal was kept horizontal. The transmitted Ar ions were charge-separated by a magnet at 130 cm downstream of the crystal, and were detected by a 2D-PSD placed at 430 cm downstream of the magnet. A Si(Li) detector for measuring de-excitation X-rays was located at an angle of  $41^\circ$  with respect to the beam direction on the horizontal plane. Through the Lorentz transformation, the angle of  $41^\circ$  in the laboratory frame corresponds to  $84.4^\circ$  in the projectile frame, i.e., nearly perpendicular to the beam direction. The area of the Si(Li) detector is 30  $\text{mm}^2$ , and the geometrical efficiency is  $2.2 \times 10^{-4}$ . The resolution for Mn  $K\alpha$  X-ray (5.9 keV) is 160 eV. An Al foil with 2  $\mu\text{m}$  thickness was placed in front of the detector as an absorber to reduce the background in the low energy region. The primary beam intensity was monitored by measuring  $K\alpha$  X-rays from a Cu foil placed at the end of the beam line by another Si(Li) detector. The beam intensities for X-ray and charge state measurements were  $\sim 10^6$  and  $\sim 10^3 \text{ s}^{-1}$ , respectively.

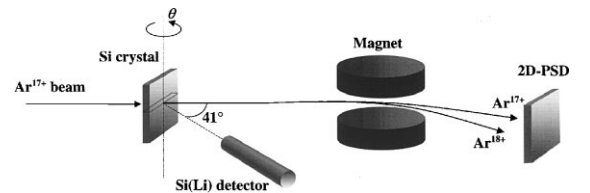


Fig. 1. A schematic drawing of the experimental set-up. A Si crystal is mounted so that the ( $2\bar{2}0$ ) plane is horizontal. A Si(Li)-detector is located on the horizontal plane.

### 3. Results and discussion

The X-ray energy spectra for random incidence, channeling (off-resonance) and RCE condition are shown in Fig. 2. Si K X-rays are seen at 1.7 keV. De-excitation X-rays from  $\text{Ar}^{17+}$  ions (3.3 keV in the projectile frame) are shifted to 5.0 keV because of the Doppler effect of the relativistic projectile velocity. Under the channeling condition, the yield of the de-excitation X-rays from the Ar ions increases compared with the random incidence because of small probability of ionization of the projectile ions due to collisions with the target atom. Under the RCE condition, the yield of the de-excitation X-rays are further enhanced.

We obtained the resonance profile for de-excitation X-rays as well as the charge state profile as shown in Fig. 3. The abscissa is the tilt angle from

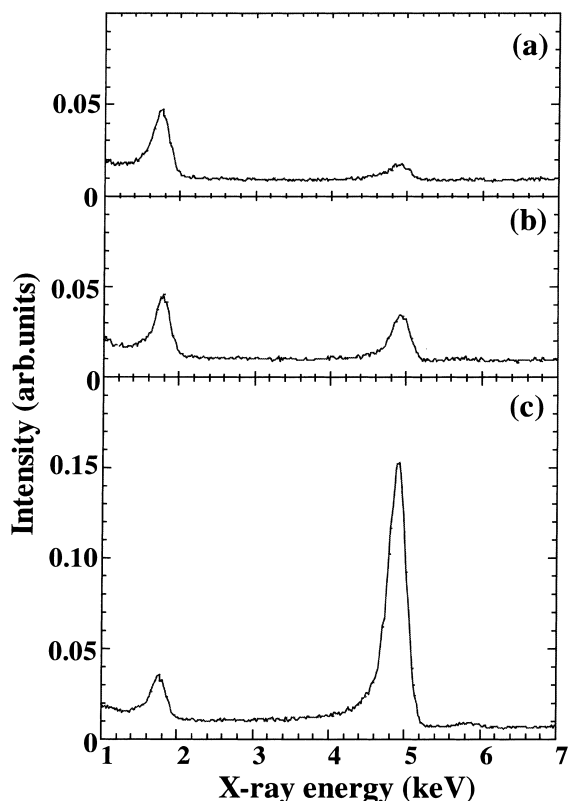


Fig. 2. X-ray spectra for (a) random incidence, (b) channeling (off-resonance) and (c) RCE condition.

the Si [1 1 0] axis. The upper scale is the transition energy corresponding to the tilt angle with the relation of Eq. (1). The X-ray resonance profile in Fig. 3(a) has two peaks similarly seen in the charge state profile in Fig. 3(b). The right peak in the X-ray profile becomes to be about six times larger than at the off-resonance condition. However, the left peak is suppressed compared with the right peak, and the doublet structure of the left peak seen in the charge state profile vanishes.

While the fraction of ionized  $\text{Ar}^{18+}$  after transmission through the Si crystal for the random incidence is 99.5%, the fraction under the channeling condition amounts to 60%. On resonance, however, the fraction of  $\text{Ar}^{18+}$  increases to 80% at the peak position as seen in Fig. 3(b). The two

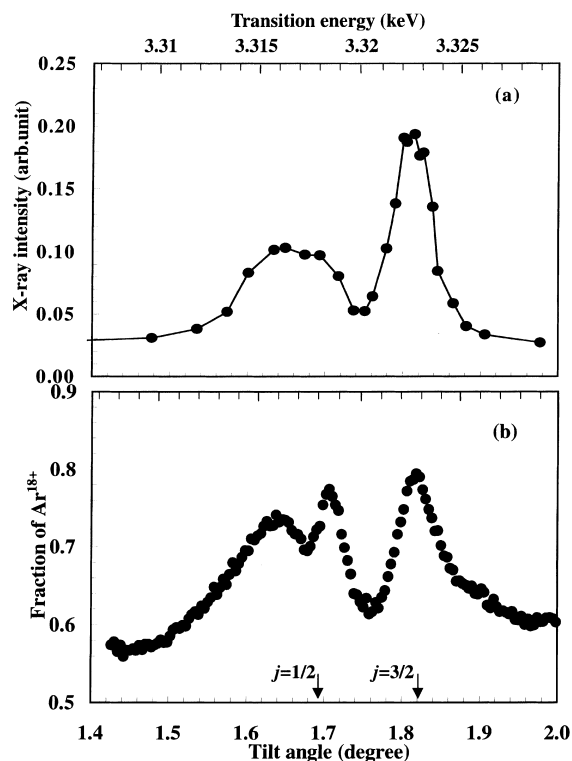


Fig. 3. Resonance profiles of  $(k, l) = (1, 1)$  RCE for (a) de-excitation X-rays and (b) charge state. The lower scale is the tilt angle from the [1 1 0] axis on the  $(2 \bar{2} 0)$  plane, and the upper scale is the transition energy corresponding to the tilt angle. Arrows indicate the position for 1s-2p transitions ( $j = 1/2$  and  $j = 3/2$ ) in vacuum.

peaks of the resonance profile reflect the spin–orbit split in  $n = 2$  states. Arrows indicate the  $1s$ – $2p$  ( $j = 1/2$  and  $j = 3/2$ ) transition energies of  $\text{Ar}^{17+}$  in vacuum. A doublet structure of the left peak is due to Stark effect originating in the crystal field. It is noted that the doublet is clearly observed compared with the case for a  $95 \mu\text{m}$  thick Si crystal [10–12].

The transition energy from  $1s$  to  $n = 2$  states in the crystal field was calculated by the perturbation theory considering the Lamb shift of the  $1s(1/2)$  and  $2s(1/2)$  states [11].<sup>1</sup> The transition energy as a function of the distance from the channel center is shown in Fig. 4. The  $n = 2$  states are split into four levels, which are hereafter named Level 1, 2, 3 and 4 in the order of increasing the transition energy. The left peak in the resonance profile corresponds to the transition to Level 1 and 2, and the right peak corresponds to Level 3 and 4. As the ion approaches to the channel center, the transition probability of the RCE becomes smaller because of the weak perturbation from the crystal potential. The small transition probability in the vicinity of the channel plane and the wide splitting between Level 1 and 2 are responsible for the doublet formation of the left peak in the charge state profile in Fig. 3(b). Moreover, the left side of the doublet peak is slightly lower than the other peaks, which reflects the steeper slope of Level 1 seen in Fig. 4. The level split between Level 3 and 4 is so narrow that the split was not observed in this measurement.

The wave functions of Levels 1–4 are expressed as linear combinations of  $2s$ ,  $2p_x$ ,  $2p_y$  and  $2p_z$  states. The fractions of  $2s$ ,  $2p_x$ ,  $2p_y$  and  $2p_z$  in these Levels as a function of the distance from the channel center are shown in Fig. 5. Here,  $x$ -axis is defined to be perpendicular to the channel plane, and  $z$ -axis is parallel to the beam direction. While the energy eigenvalues of  $n = 2$  states are little changes by including the  $2s(1/2)$  Lamb shift, the wave functions of Level 1 and 2 are drastically altered at the small distance from the channel

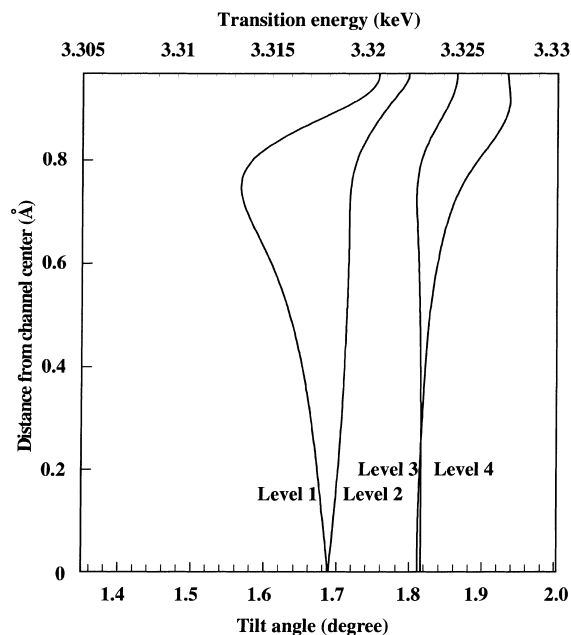


Fig. 4. Calculated transition energy from  $1s$  to  $n = 2$  states as a function of the distance from the channel center. Four levels are named as Level 1, Level 2, Level 3 and Level 4 from the lower transition energy.

center (compare Fig. 5 with Fig. 3 of [11]). This behavior is attributed to the fact that the expected energy for  $2s(1/2)$  is lower than that for  $2p(1/2)$  at the channel center without the  $2s(1/2)$  Lamb shift because of the curvature of the crystal potential, however, it becomes higher including the Lamb shift. The dominant component in Level 1 and 2 is the  $2s$  state, which does not decay via a single photon emission. The lifetime of an  $n = 2$  state with the large fraction of the  $2s$  component becomes much longer, and excited ions to Level 1 and 2 do not decay in a field of view of the Si(Li) detector. This situation results in the suppression of left peak for the X-ray resonance profile. Moreover, from the fact that the channeled ions maintain the information of the initially excited state, it is considered that the transition between  $n = 2$  states by electron or nuclear impact, which tends to smear out the information of the initially excited level, does not occur so frequently.

Here, in order to discuss the evolution of the electronic states resulting from the fundamental processes under the RCE condition, several

<sup>1</sup> The  $2s(1/2)$  and  $2p(1/2)$  Lamb shift are taken into account in the present calculation, however, the  $2s(1/2)$  Lamb shift was not taken into account in the calculation in [11].

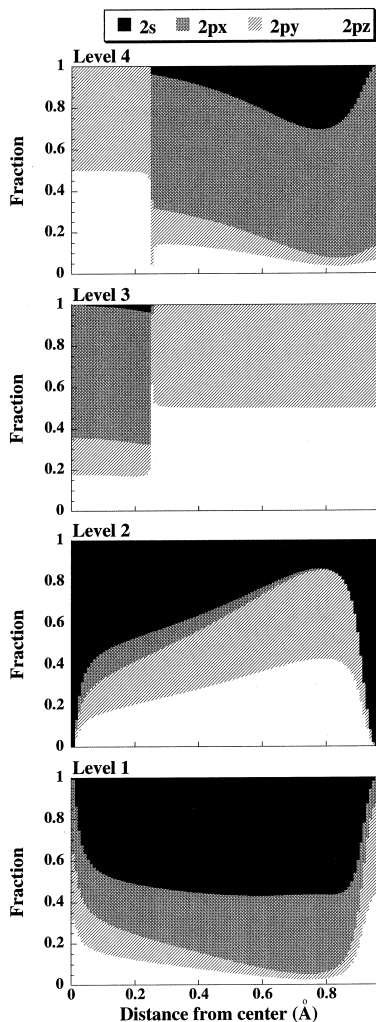


Fig. 5. Fractions of 2s, 2p<sub>x</sub>, 2p<sub>y</sub>, and 2p<sub>z</sub> components in Level 1–4 as a function of the distance from the channel center.

parameters are introduced, i.e., mean-free-paths of 2p-ionization,  $\lambda_i$  and 2p-1s de-excitation,  $\lambda_x$ . For more detailed discussion about the X-ray resonance profile, a period and a phase of the Rabi-oscillation of the resonant coherent excitation and de-excitation processes have to be taken into account. However, the main feature of the X-ray resonance profile can be qualitatively explained by the mean-free-paths,  $\lambda_i$  and  $\lambda_x$ . Ionization probabilities from 2p-substates, i.e., 2p<sub>x</sub>, 2p<sub>y</sub> and 2p<sub>z</sub> are different from each other when we consider the electron flux and density in the crystal. We,

nevertheless, assume that they are identical because the size of the Ar<sup>17+</sup> ion is much smaller than the inter-planar distance of the (2  $\bar{2}$  0) channel (= 1.92 Å). The value of  $\lambda_i$  for the best channeled ions traveling in the channel center is estimated to be  $\sim 60 \mu\text{m}$  from the local electron density calculated from the Molière potential and the electron impact ionization cross section [13]. The value of  $\lambda_i$  for the channeled ions with the oscillation amplitude of 0.72 Å, which is three-quarter of the distance between the channel center and plane, is estimated to be  $\sim 1.6 \mu\text{m}$ . For the channeled ions with the large oscillation amplitude, the nuclear impact contributes to the ionization to a large extent. The impact parameter dependence of ionization by nuclear impact is estimated from the experimental result of the fraction of ionized Ar<sup>18+</sup> ions as a function of the energy loss [10–12]. Most of de-excitation occurs inside the Si crystal, because  $\lambda_x$  is  $\sim 4.6 \mu\text{m}$  [14]. It is noted that  $\lambda_x$  is independent of the distance from the channel center.

For the best channeled ions, most of excited ions to  $n = 2$  states decay with the X-ray emission, because the  $\lambda_i$  is more than ten times larger than  $\lambda_x$ . On the other hand, the  $\lambda_i$  is three times smaller than  $\lambda_x$  for channeled ions with the large oscillation amplitudes of 0.72 Å. Therefore, excited ions with large oscillation amplitude are easily ionized, and the channeled ions with small oscillation amplitudes mainly contribute to the X-ray resonance profile. As the result, the doublet structure of the left peak as seen in the charge state resonance profile vanishes in the X-ray profile. In the previous experiment with a 95  $\mu\text{m}$  thick Si crystal [10–12], the doublet structure of the left peak in the charge state profile was not clearly observed. The reason why the doublet structure is well resolved compared with the thicker crystal is also explained by this picture. The crystal thickness of 95  $\mu\text{m}$  is larger than the  $\lambda_i$  for the best channeled ions, and excited ions to  $n = 2$  state are eventually ionized even for the best channeled ions. As the result, the doublet structure did not clearly appear.

In summary, we observed the RCE through the de-excitation X-rays as well as the charge state distribution adopting a Si crystal with 21  $\mu\text{m}$  thickness. The obtained X-ray resonance profile has a different feature from the charge state

resonance profile. The suppression of the left peak in the X-ray resonance profile reflects dominance of the 2s state in Level 1 and 2. The disappearance of the doublet structure in the X-ray profile is owing to the small ionization probability of the channeled ions with a small oscillation amplitude.

### Acknowledgements

This investigation is in part supported by Matsuo Foundation, the Sumitomo Foundation, the Mitsubishi Foundation, and also a Research Project with Heavy Ions at NIRS-HIMAC. We owe to Dr. M. Sataka at JAERI and Dr. T. Kambara at RIKEN for the use of Si(Li) detectors in the present experiment.

### References

- [1] V.V. Okorokov, JETP Lett. 2 (1965) 111.
- [2] V.V. Okorokov, Sov. J. Nucl. Phys. 2 (1966) 719.
- [3] S. Datz, C.D. Moak, O.H. Crawford, H.F. Krause, P.F. Dittner, J. Gomez del Campo, J.A. Biggerstaff, P.D. Miller, P. Hvelplund, K. Knudsen, Phys. Rev. Lett. 40 (1978) 843.
- [4] H.F. Krause, S. Datz, Adv. Atomic Mol. Opti. Phys. 37 (1996) 139.
- [5] J.U. Andersen, G.C. Ball, J. Chevallier, J.A. Davies, W.G. Davies, J.S. Forster, J.S. Geiger, H. Geissel, Nucl. Instr. and Meth. B 119 (1996) 292.
- [6] F. Fujimoto, K. Komaki, A. Ootuka, E. Vilalta, Y. Iwata, Y. Hirao, T. Hasegawa, M. Sekiguchi, A. Mizobuchi, T. Hattori, K. Kimura, Nucl. Instr. and Meth. B 22 (1988) 354.
- [7] Y. Iwata, K. Komaki, Y. Yamazaki, M. Sekiguchi, T. Hattori, T. Hasegawa, F. Fujimoto, Nucl. Instr. and Meth. B 48 (1990) 163.
- [8] S. Datz, P.F. Dittner, J. Gomez del Campo, K. Kimura, H.F. Krause, T.M. Rosseel, C.R. Vane, Y. Iwata, K. Komaki, Y. Yamazaki, F. Fujimoto, Y. Honda, Radiat. Eff. Def. Solids 117 (1991) 73.
- [9] S. Datz, P.F. Dittner, H.F. Krause, C.R. Vane, O.H. Crawford, J.S. Forster, G.S. Ball, W.G. Davies, J.S. Geiger, Nucl. Instr. and Meth. B 100 (1995) 272.
- [10] T. Azuma, T. Ito, K. Komaki, Y. Yamazaki, M. Sano, M. Torikoshi, A. Kitagawa, E. Takada, T. Murakami, Phys. Rev. Lett. 83 (1999) 528.
- [11] K. Komaki, T. Azuma, T. Ito, Y. Takabayashi, Y. Yamazaki, M. Sano, M. Torikoshi, A. Kitagawa, E. Takada, T. Murakami, Nucl. Instr. and Meth. B 146 (1998) 19.
- [12] T. Azuma, T. Ito, Y. Yamazaki, K. Komaki, M. Sano, M. Torikoshi, A. Kitagawa, E. Takada, T. Murakami, Nucl. Instr. and Meth. B 135 (1998) 61.
- [13] J.P. Rozet, C. Stéphan, D. Vernhet, Nucl. Instr. and Meth. B 107 (1996) 67.
- [14] H.A. Bethe, E.E. Salpeter, Quantum Mechanics of One- and Two-Electron Atoms, 1957.